arXiv:1406.1465v1 [astro-ph.GA] 5 Jun 2014

The formation of massive primordial stars in the presence of moderate UV backgrounds

M. A. Latif [1], D. R. G. Schleicher [1], S. Bovino [1], T. Grassi [2,3], M. Spaans[4]
Institut für Astrophysik, Georg-August-Universität, Friedrich-Hund-Platz 1, 37077 Göttingen, Germany
Centre for Star and Planet Formation, Natural History Museum of Denmark, Øster Voldgade 5-7, DK-1350 Copenhagen, Denmark
Niels Bohr Institute, University of Copenhagen, Juliane Maries Vej 30, DK-2100 Copenhagen, Denmark
Kapteyn Astronomical Institute, University of Groningen, The Netherlands
mlatif@astro.physik.uni-goettingen.de

ABSTRACT

Radiative feedback from populations II stars played a vital role in early structure formation. Particularly, photons below the Lyman limit can escape the star forming regions and produce a background ultraviolet (UV) flux which consequently may influence the pristine halos far away from the radiation sources. These photons can quench the formation of molecular hydrogen by photo-detachment of H^-. In this study, we explore the impact of such UV radiation on fragmentation in massive primordial halos of a few times 10^7 $M_\odot$. To accomplish this goal, we perform high resolution cosmological simulations for two distinct halos and vary the strength of the impinging background UV field in units of J_{21}. We further make use of sink particles to follow the evolution for 10,000 years after reaching the maximum refinement level. No vigorous fragmentation is observed in UV illuminated halos while the accretion rate changes according to the thermal properties. Our findings show that a few 100-10, 000 solar mass protostars are formed when halos are irradiated by $J_{21} = 10 - 500$ at $z > 10$ and suggest a strong relation between the strength of UV flux and mass of a protostar. This mode of star formation is quite different from minihalos, as higher accretion rates of about $0.01 - 0.1$ $M_\odot$/yr are observed by the end of our simulations. The resulting massive stars are the potential cradles for the formation of intermediate mass black holes at earlier cosmic times and contribute to the formation of a global X-ray background.

Subject headings: methods: numerical – cosmology: theory – early Universe – galaxies: formation

1. Introduction

The first generation of stars so-called population III stars ushered the Universe out of the cosmic dark ages and brought the first light in the cosmos. They are presumed to be assembled in dark matter halos of $10^5 - 10^6$ $M_\odot$ at $z = 20 - 30$ (Abel et al. 2002; Johnson & Khochfar 2011; Clark et al. 2011; Greif et al. 2012; Stacy et al. 2012; Latif et al. 2013c; Bovino et al. 2014) and influenced the subsequent structure formation via mechanical, chemical and radiative feedback (Ciardi & Ferrara 2005; Schleicher et al. 2008; Latif et al. 2012; Maio et al. 2011). Pop III stars enriched the intergalactic medium with metals and led to the second generation of stars known as Pop II stars. According to the hierarchical paradigm of structure formation, the first galaxies are formed in massive primordial halos of $10^7 - 10^8$ $M_\odot$ at about $z = 15$ most likely hosting both stellar populations (Greif et al. 2008; Wise et al. 2008; Bromm et al. 2009; Latif et al. 2011a).

During the epoch of reionization, radiation emitted by the Pop II stars not only photo-ionized the gas but also photo-dissociated H_2 and HD molecules. The molecular hydrogen is the only coolant in primordial gas which can bring the gas temperature down to few hundred K and may induce star formation. In the presence of an intense UV flux, the formation of H_2 remains suppressed (due to photo-detachment of H^- which is the main pathway of H_2

formation) in pristine halos. Under these conditions, cooling only proceeds via Lyman alpha radiation in massive primordial halos of 10^7 – 10^8 $M_\odot$ and massive objects are expected to form and are known as direct collapse black holes (DCBHs) (Oh & Haiman 2002; Spaans & Silk 2006; Begelman et al. 2006; Lodato & Natarajan 2006; Volonteri 2010; Schleicher et al. 2010; Latif et al. 2011b; Johnson et al. 2011; Volonteri & Bellovary 2012; Haiman 2012; Prieto et al. 2013; Latif et al. 2013a; Whalen et al. 2013a; Aykutalp et al. 2013; Latif et al. 2013e; Yue et al. 2014; Latif et al. 2014b; Inayoshi et al. 2014).

The formation of DCBHs requires a critical strength of UV flux above which halos remain H_2 free (Omukai 2001; Shang et al. 2010; Latif et al. 2014a; Johnson et al. 2014). Such a UV flux can only exist in the close vicinity of star forming galaxies (Dijkstra et al. 2008; Agarwal et al. 2012, 2014; Dijkstra et al. 2014) and the mass scales of the resulting stars have been explored in recent studies. In fact, high resolution numerical simulations show that supermassive stars of $\sim$ 10^5 $M_\odot$ form in the presence of strong UV flux (Bromm & Loeb 2003; Wise et al. 2008; Regan & Haehnelt 2009; Latif et al. 2011b, 2013d,b,a,e; Regan et al. 2014) and agree with theoretical predictions (Begelman et al. 2008; Begelman 2010; Ball et al. 2011; Hosokawa et al. 2012; Ball et al. 2012; Schleicher et al. 2013; Hosokawa et al. 2013; Whalen et al. 2013b). Employing a cosmological framework following the formation and accretion of the resulting supermassive objects, Ferrara et al. (2014) have derived detailed predictions on the mass function of the first high-mass black holes.

On the other hand, moderate strengths of the background UV flux may occur more often during the epoch of reionization without requiring the presence of nearby sources. In the ubiquity of such moderate UV fluxes, the formation of H_2 does occur and may lead to star formation. Particularly, during the epoch of reionization the dominant background flux is emitted by Pop II stars. The strength of such UV flux to dissociate H_2 formation was quantified in a recent study by Latif et al. (2014a) and found that J_{21}^{crit} ranges from 400-700 higher than previous estimates. Therefore, halos exposed below J_{21}^{crit} are expected to be more abundant, for J_{21} = 10 the fraction of halos is seven orders of magnitude higher compared to the J_{21} = 500 (see figure C1 of Dijkstra et al. 2014). Thus it is desirable to explore the typical mass scales of stars forming in halos illuminated by moderate UV fluxes emitted by Pop II stars. Safranek-Shrader et al. (2012) have performed three dimensional simulations to study the fragmentation in massive halos irradiated by Lyman-Werner flux of strength J_{21} = 100 for T_* = 10^5 K and found that a dense turbulent core of 10^4 $M_\odot$ forms in the center of the halo.

In this study, we explore the mass scales of stars formed under the moderate strengths of the background UV flux. To achieve this goal, we perform three dimensional cosmological simulations for two halos of a few times 10^7 $M_\odot$ and vary the strength of UV flux (hereafter called J_{21}, i.e. UV flux with energy below 13.6 eV). We employed a Jeans resolution of 32 cells during the course of simulations and make use of sink particles to follow the evolution for 10, 000 years after reaching the maximum refinement level in simulations. The main objective of this work is to determine the mass scale of stars for a moderate UV radiation field. This has potential implications for the formation of intermediate mass black holes in stellar clusters at earlier cosmic times. We note that the expected ionizing UV feedback by these protostars is still weak for accretion rates higher than 0.1 $M_\odot$/yr (Schleicher et al. 2013; Hosokawa et al. 2013).

The outline of this article is as follows. In section 2, we describe our numerical methodology and give a brief overview of chemical network. We present our main results in section 3 and confer our conclusions in section 4.

2. Computational methods

We employed the open source code ENZO [1] to perform three dimensional cosmological simulations following the collapse in massive primordial halos (Bryan et al. 2014). ENZO is an adaptive mesh refinement, parallel, Eulerian code. It makes use of the piece-wise parabolic method to solve the hydrodynamical equations. The dark matter dynamics is solved by using the particle-mesh technique.

Our simulations are started with cosmological initial conditions at z = 100. We first run simulations with a uniform grid resolution of 128^3 cells and select the most massive DM halos in a computational domain with comoving size of 1 Mpc/h. The simulations are commenced with two additional nested refinement levels each with a resolution of 128^3 cells in addition to a top grid resolution of 128^3 cells and are centered on

[1] http://enzo-project.org/, changeset:48de94f882d8

the most massive halo. We employed 5767168 particles to solve the dark matter dynamics. To follow the collapse of a halo additional 18 levels of refinement are applied during the course of simulations with a fixed Jeans resolution of 32 cells. We further make use of sink particles to follow the accretion for 10,000 years after the formation of the first sink. Detailed discussions about the sinks particles and the simulation setup can be found in our previous studies (Latif et al. 2013a,e,b, 2014c).

To follow the evolution of chemical species, the rate equations of the following species H, H^+, He, He^+, He^{++}, e^-, H^-, H_2, H_2^+ are solved in our cosmological simulations. We used publicly available KROME package[2] (Grassi et al. 2014) to compute the evolution of chemical and thermal processes. The chemical network and the microphysics employed here are the same as in Latif et al. (2014a) , including the self-shielding model from Wolcott-Green et al. (2011). We have not included HD chemistry in our simulation as HD is very fragile molecule and even weaker flux such as $J_{21} = 0.1$ is found to be sufficient to dissociate it. The same was observed in simulations of Safranek-Shrader et al. (2012).

In this study, simulations are performed for two distinct halos by varying the strength of UV flux below the Lyman limit. The properties of simulated halos and the strength of UV flux in units of J_{21} are listed in table 1.

3. Main Results

In total, we have performed six cosmological simulations for two different halos of a few times 10^7 $M_\odot$ and varied the strength of J_{21} (i.e. 10, 100 and 500). Our results show that initially the gas is heated up to 10^4 K in the presence of the background UV flux and then cools by Lyman alpha cooling. Depending on the strength of the UV flux, H_2 formation takes place and cooling due to the molecular hydrogen becomes effective. For $J_{21} = 10$, 100, the central temperature in the halo is about 1000 K while for $J_{21} = 500$ the temperature in the core is a few thousand K as shown in figure 1. It is also found that for a weaker flux (i.e. $J_{21} = 10$), H_2 cooling kicks in at densities around 10^{-23} g/cm^3 while for $J_{21} = 100$ it becomes effective around 10^{-20} g/cm^3. For the strongest flux, it starts at even higher densities of about 10^{-18} g/cm^3.

[2]Webpage KROME: www.kromepackage.org

The density structure for various strengths of the UV field is shown in figure 2. It can be seen that for $J_{21} = 10$ the gas in the halos becomes more clumpy and indicates the possibility to form multiple clumps. These clumps are formed by locally induced H_2 cooling which lowers the gas temperature down to a few hundred K as shown in figures 3 and 4. For $J_{21} = 10$, the clumps with no sinks are gravitational unbound and have masses of the order of few solar masses. For $J_{21} = 100$, the halos have less structure and the number of cold clumps is reduced. This is due to the fact that the overall temperature in the halo is higher particularly in the outskirts which suppresses fragmentation. Similarly, the fraction of molecular hydrogen is significantly reduced in the surrounding of the halo. For the strongest flux ($J_{21} = 500$), there is no sign of fragmentation as the central temperature in the halos is a few thousand K and in one halo later approaches an isothermal state due to the temperature dependence of the H_2 collisional dissociation rate (Martin et al. 1996). The fraction of molecular hydrogen is significantly lower and is limited to only core of the halos.

To further quantify the masses of the clumps formed in our simulated halos, we employed sink particles which represent the protostars in our simulations and followed the evolution for many free-fall times. The masses of the sinks are listed in table 1. It is found that for $J_{21} = 10$, the masses of the sinks are a few hundred to about 1500 $M_\odot$. In halo A two sinks are formed. For $J_{21} = 100$, only one massive sink is formed in each halo and their masses are 7400 and 2500 $M_\odot$. The masses of the sinks are above 22, 000 solar masses for the strongest flux case and a single sink is formed per halo. Overall, our results suggest that fragmentation in the halos is reduced by increasing the strength of background UV flux according to the theoretical expectations. For $J_{21} = 10$ and 100, although the central temperatures are quite similar the masses are higher by a factor of a few for $J_{21} = 100$. This is because of the warmer gas in the surroundings of the halo which leads to higher accretion rates and consequently higher sink masses at the end of our simulations. It is found that the masses of the sinks in halo B are about a factor of two lower compared to halo A. Overall, the average density in halo B is lower and has a higher rotational support. This leads to lower accretion rates in halo B and consequently lower sink masses.

The physical properties of the halos are depicted in figures 5 and 6. The maximum density in the halos

Table 1: Properties of the simulated halos for J_{21} are listed here.

Model No	J_{21} in units of J_{21}	Mass $M_\odot$	Redshift z	spin parameter λ	Sink particle masses $M_\odot$
A				0.034	
	10	4.3×10^7	10.98		1461, 231
	100	5.45×10^7	10.63		7337
	500	5.47×10^7	10.60		22739
B				0.03	
	10	2.9×10^7	11.73		623
	100	3.2×10^7	11.38		2592
	500	3.2×10^7	11.20		24785

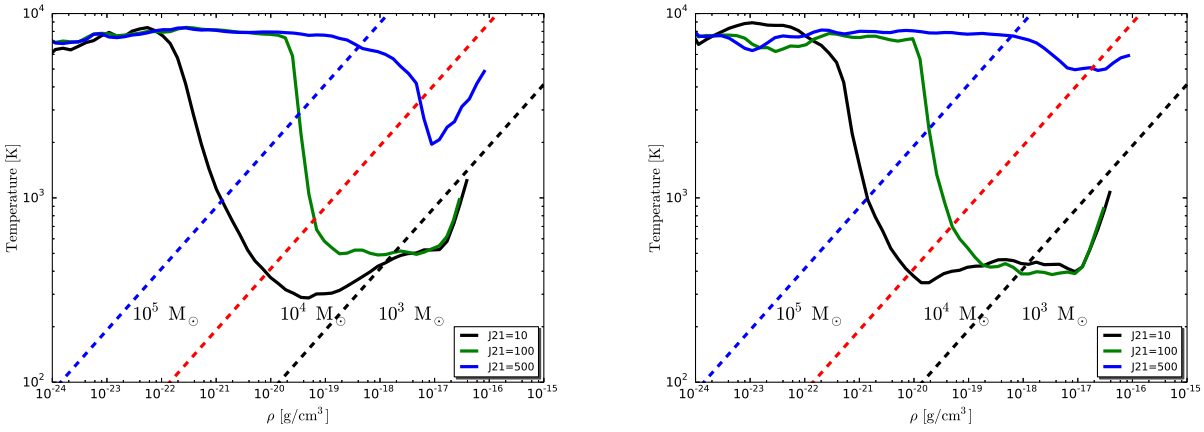

Fig. 1.— Averaged values of temperature are plotted against density at the end point of our simulations for various strengths of J_{21}. The left panel shows halo A and the right panel stands for halo B. The dashed lines show the expected thermal Jeans mass at these scales.

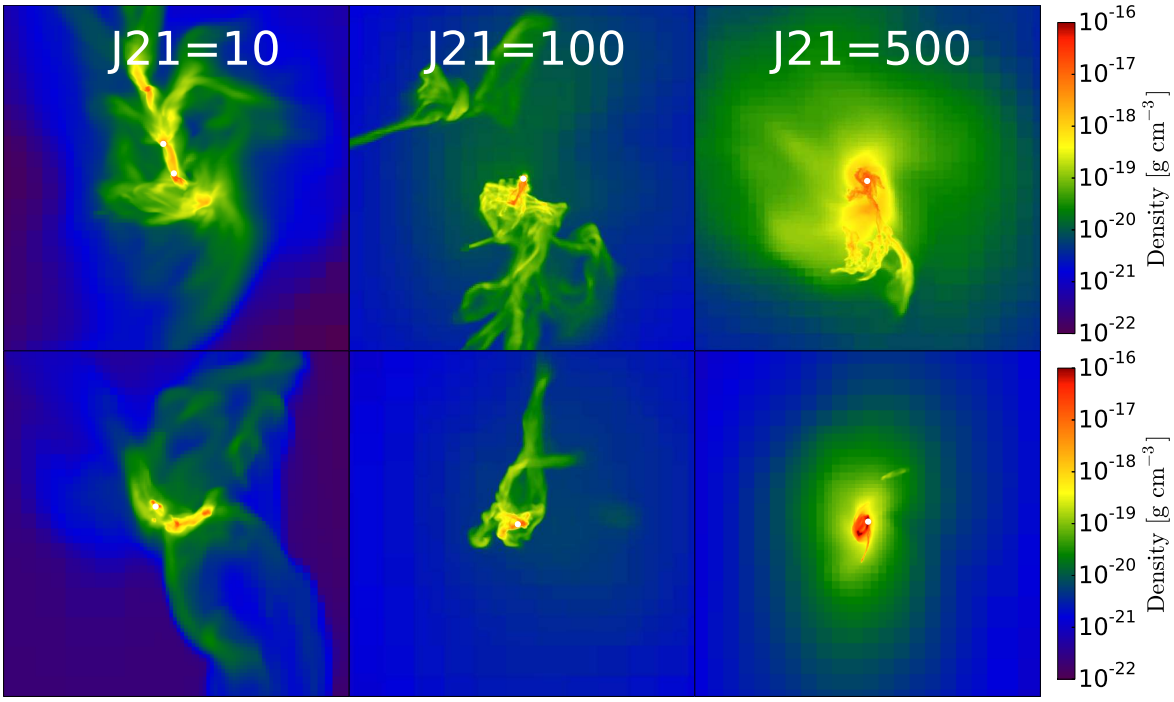

Fig. 2.— The final state of our simulation is represented by the average density along the line of sight for different radiation backgrounds. The top panel represents halo A and the bottom panel halo B. The overplotted white points depict sink particles. The masses of the sink particles are listed in table 1.

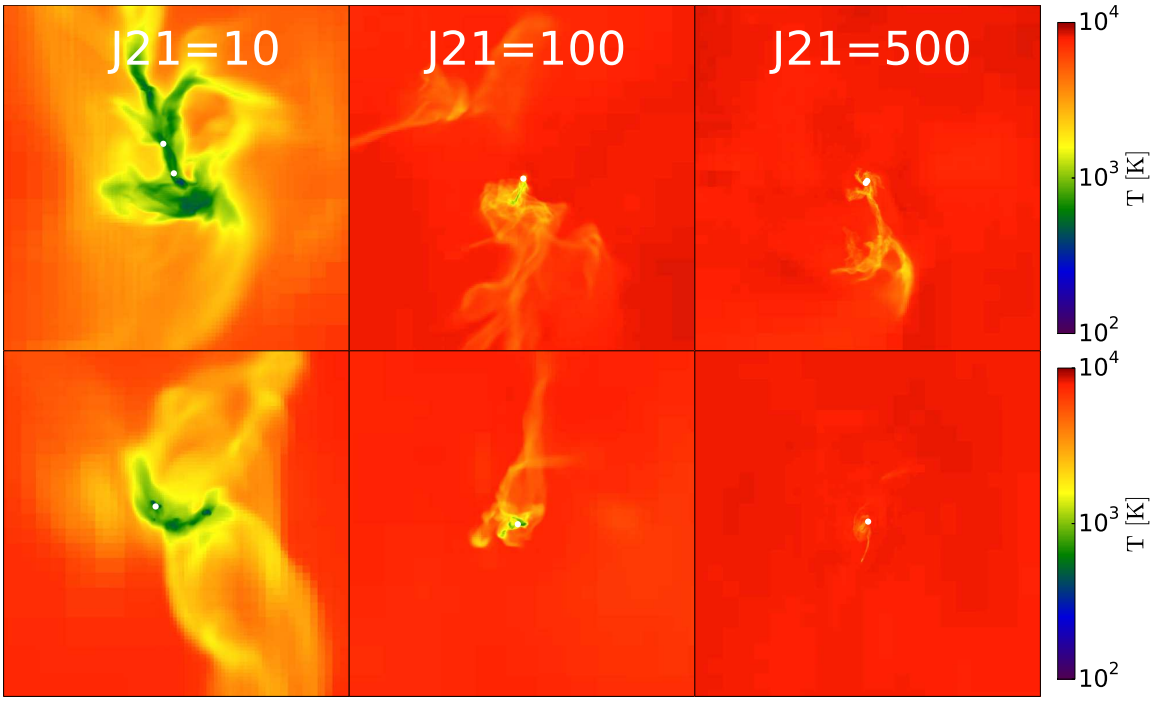

Fig. 3.— Temperature is shown here corresponding to the figure 4.

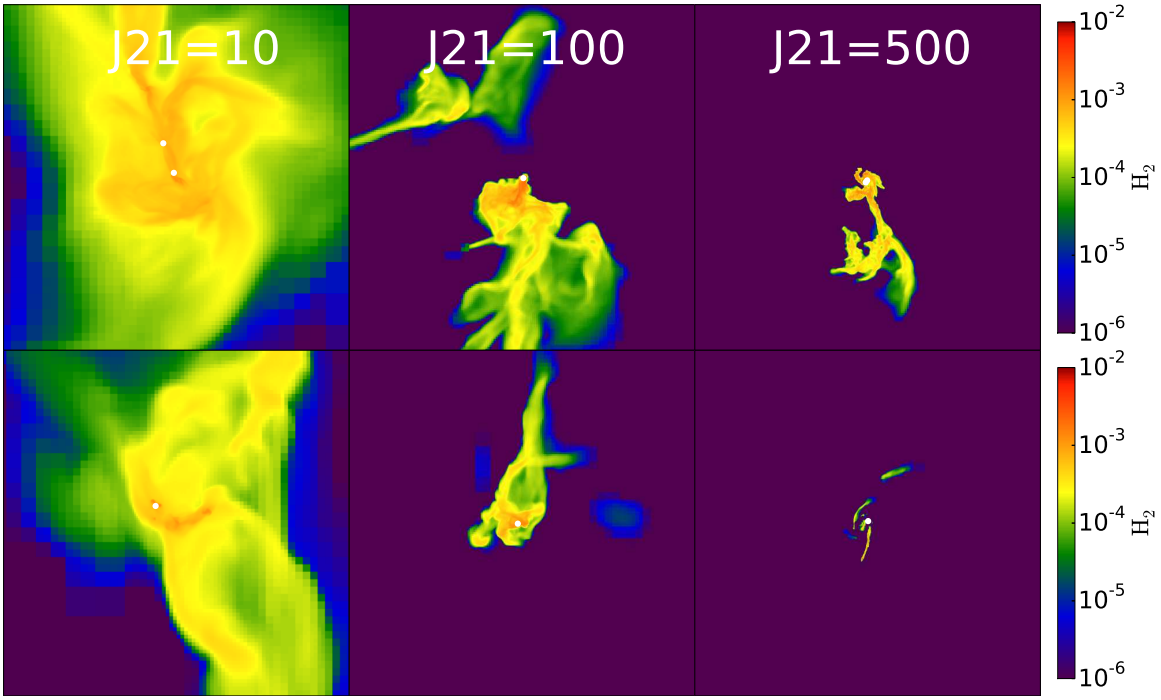

Fig. 4.— The abundance of molecular hydrogen is depicted here same as figure 4.

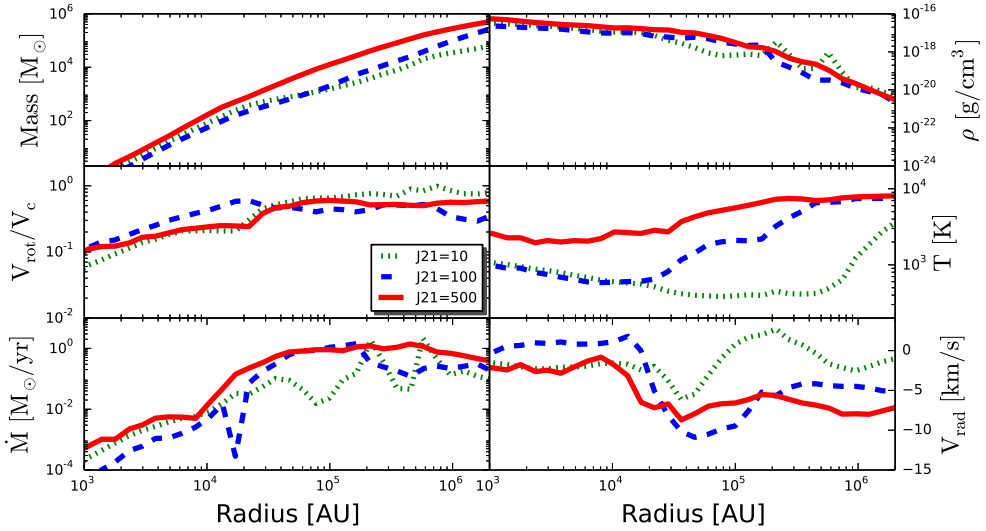

Fig. 5.— Radially averaged spherically binned profiles are shown here for halo A at the end point of our simulations. Each line style represents a different strength of the UV flux as shown in the legend. The top panels show the mass and density, the middle panels show the ratio v_{rot}/v_c and the temperature, and the bottom panels show the mass accretion rates and infall velocities.

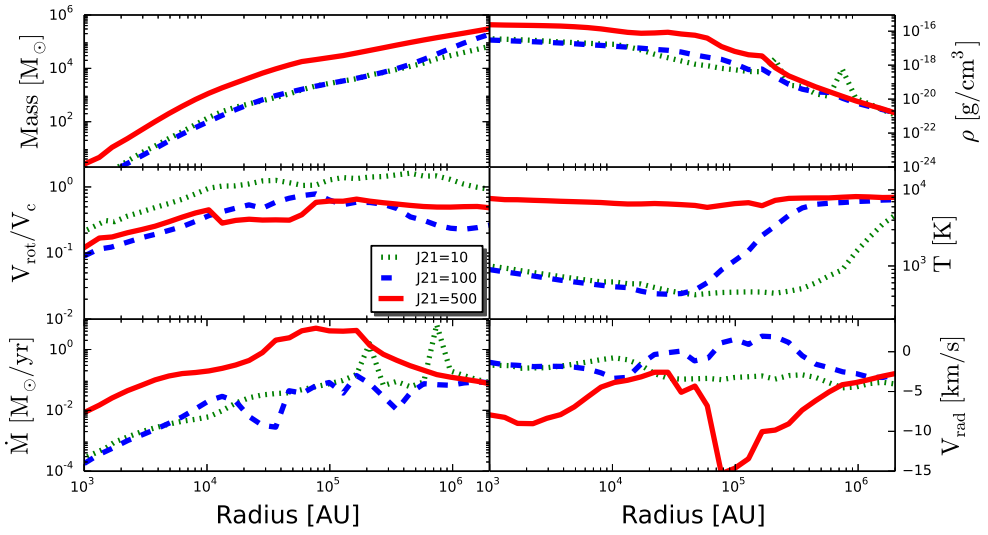

Fig. 6.— Same as figure 5 but for halo B.

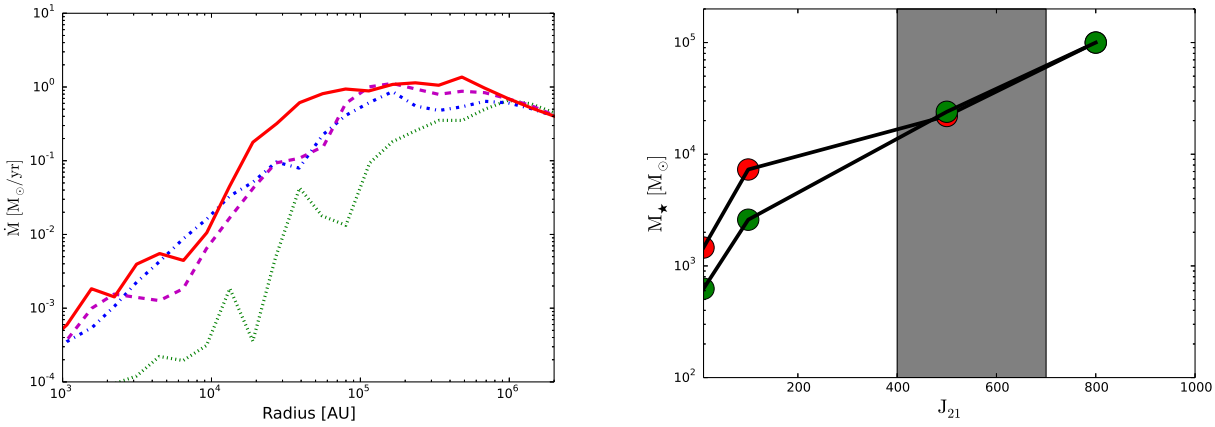

Fig. 7.— The left panel shows the time evolution of the mass accretion rates against radius. The green line shows mass accretion rates at the formation of sink while the red line depicts evolution for 10,000 years for J_{21} = 500. The right panel shows the expected stellar masses for various strengths of the background UV flux below the Lyman limit. The dashed vertical shaded region represents the range of critical values. The blue and red spheres represent halo A and B. The last two data points are taken from Latif et al 2013e and just indicate the expected masses for J_{21} higher than critical values.

is 10^{-16} g/cm^3. The density profile follow an R^{-2} behavior at larger radii for almost all fluxes and becomes flat in the core of the halo corresponding to the Jeans length. The deviations from this behavior are observed for weaker values of J_{21} due to the additional substructure inside the halo. The difference between weaker and strongest flux are more prominent in halo B as it collapses almost isothermally for $J_{21} = 500$. The overall density in halo B is lower by a factor of a few compared to the halo A around 10 pc. For $J_{21} = 10$, cooling due to H_2 becomes effective in the central 10 pc of the halo. On the other hand for $J_{21} = 100$ it is limited to the central pc of the halo while for $J_{21} = 500$ cooling due to the molecular hydrogen is not very effective due to its lower abundance.

The impact of different thermal evolutions is also reflected in the infall velocities of the halos. Higher temperatures lead to higher infall velocities and also indicate lower molecular hydrogen fractions in those halos. Similarly lower infall velocities are observed for the weaker fluxes indicating that the halo is in the molecular cooling phase. Halo B has lower radial infall velocities compared to halo A. Large accretion rates of about 0.1 $M_\odot$/yr are observed. The decline in accretion rates towards the center is due to the increasing pressure support within the Jeans length. It is further found that the accretion rates are slightly higher for stronger fluxes and are lower in halo B compared to halo A. The enclosed mass in the halos is higher for stronger fluxes. This is due to the higher infall velocities and higher accretion rates for these cases. It is also found that halo B has higher rotational support. We further noted that the accretions rates increased during the course of simulations and are shown for a representative case in figure 7.

We show the expected stellar masses for various values of J_{21} in figure 7. It is observed that the stars formed in the presence of UV feedback are very massive typically above one thousand solar masses. This figure shows an increase in the stellar masses with the strength of the UV flux, i.e. the higher the UV flux the more massive the star. Fragmentation may occur at larger scales but may not be able to prevent the formation of massive stars. We expect that these massive to supermassive stars are the potential candidates for the formation of intermediate to supermassive black holes.

4. Discussion and conclusions

In this article, we explored fragmentation in massive primordial halos of a few times 10^7 $M_\odot$ irradiated by different UV fluxes below the Lyman limit. To achieve this goal, we performed high resolution cosmological simulations for two distinct halos collapsing at $z > 10$ and varied the strength of the UV flux from 10-500 in units of J_{21}. We exploited the adaptive mesh refinement technique to follow the collapse of the halo by employing additional 18 dynamical refinement levels during the course of simulations which yields an effective resolution of about 100 AU. To further follow the evolution for longer time scales, sink particles representing protostars were employed. A fixed Jeans resolution of 32 cells were mandated during the entire course of simulations.

Our findings show that the formation of H_2 gets delayed and no strong fragmentation occurs in the halos illuminated by the UV flux of 10-500 in units of J_{21}. For $J_{21} = 10$, in our simulated halos binary or multiple systems may likely form but for higher values of J_{21} only one single object is formed. At the end of our simulations, massive protostars of a few 100-10, 000 solar masses are formed and large accretion rates of about $0.1 - 0.01$ $M_\odot$/yr are observed. These relatively high accretion rates distinguish them from normal star formation mode in minihalos. These massive stars formed in the early universe are the potential candidates for the formation of intermediate mass black holes.

H_2 cooling reaches local thermal equilibrium at densities higher than 10^4 cm^{-3} and the cooling rate scales as density while compressional heating varies with $\rho^{3/2}$. So the expected polytropic index stiffens (i.e. $\gamma > 1$) and suppresses fragmentation (Spaans & Silk 2000). Of course, the possibility of fragmentation at higher density cannot be completely ruled out and low mass stars may form in addition to the most massive object.

Safranek-Shrader et al. (2012) performed similar simulations for a halo of similar mass irradiated by the background UV flux emitted by population III stars. They also found that the gas self-shields from the UV flux and a dense core of 10^4 $M_\odot$ develops. They further used sink particles to follow the simulations for longer times and found that a massive sink of about 1000 solar masses is formed. Their study is comparable to $J_{21} = 10$ in our simulations due to the background UV flux emitted by two different stellar populations. They

have employed radiation spectrum with $T_* = 10^5$ K in their calculations which mainly dissociates the molecular hydrogen via the Solomon process and H_2 self-shielding is more important in contrast to our study.

In particular, we compare the accretion rates at the same times in both simulations and our results appear rather consistent. We note however that there is no one-to-one correspondence, as the thermal evolution does not precisely match and our halo is somewhat warmer on larger scales. In addition, there are of course fluctuations from halo to halo, so some variation between the halos is expected, as we also see here when comparing halos A and B.

To further explore the possible fragmentation at higher densities, we in total added 27 refinement levels which yield resolution down to sub AU scales (0.25 AU) and the peak densities of 10^{-11} g/cm^3. We however do not see any indication of further fragmentation for these runs. Such verification further confirms that even if fragmentation occurs at later stages the mass of central object would not change significantly. Our results for $J_{21} = 10$ are in agreement with Hirano et al. (2014) who simulated about 100 minihalos and found that even massive stars of thousand solar masses can form in the presence of similar mass accretion rates that found in this study.

We also note that our simulations do not include the ionizing UV feedback by the protostar. As long as the accretion rates remain higher than 0.1 $M_\odot$/yr, no strong feedback is expected (Hosokawa et al. 2012, 2013; Schleicher et al. 2013). Ionizing feedback may kick in once the accretion rates drop more significantly, potentially limiting the growth of the resulting objects.

We also assumed that halos are metal free and given the patchy distribution of the metal such halos may exist down to z=6 (Trenti et al. 2009). However, if metal enrichment takes places in these halos it will lead to fragmentation and most likely star cluster of low mass stars (Safranek-Shrader et al. 2014; Peters et al. 2014). Even a small amount of dust, i.e. 10^{-5} $Z/Z_\odot$ is sufficient to boost the H_2 fraction and induce fragmentation (Cazaux & Spaans 2009). In fact, recent observations suggest the potential presence of intermediate mass black holes in globular clusters (Kamann et al. 2014).

From the results given here, we deduce that massive to supermassive stars may be more common than previously expected, and can also form for radiative backgrounds $J_{21} < J_{crit}$. Based on the recent estimates of Dijkstra et al. (2014) for the expected density of halos for various UV field strengths, the expected fraction of halos exposed to $J_{21} < J_{crit}$ is few orders of magnitude higher. We expect such stars to produce a considerable amount of UV feedback once they are on the main sequence, thus considerably contributing to the ionization of their environment, and perhaps also to the epoch of reionization. At the end of their lives, they may collapse to an intermediate mass black hole, and the X-rays released during their formation may contribute to establish a global background (Yue et al. 2013).

Acknowledgments

The simulations described in this work were performed using the Enzo code, developed by the Laboratory for Computational Astrophysics at the University of California in San Diego (http://lca.ucsd.edu). We acknowledge research funding by Deutsche Forschungsgemeinschaft (DFG) under grant SFB 963/1 (project A12) and computing time from HLRN under project nip00029. DRGS and SB thank the DFG for funding via the Schwerpunktprogram SPP 1573 "Physics of the Interstellar Medium" (grant SCHL 1964/1 – 1). The simulation results are analyzed using the visualization toolkit for astrophysical data YT (Turk et al. 2011).

REFERENCES

Abel, T., Bryan, G. L., & Norman, M. L. 2002, Science, 295, 93

Agarwal, B., Dalla Vecchia, C., Johnson, J. L., Khochfar, S., & Paardekooper, J.-P. 2014, ArXiv e-prints:1403.5267

Agarwal, B., Khochfar, S., Johnson, J. L., Neistein, E., Dalla Vecchia, C., & Livio, M. 2012, MNRAS, 425, 2854

Aykutalp, A., Wise, J. H., Meijerink, R., & Spaans, M. 2013, ApJ, 771, 50

Ball, W. H., Tout, C. A., & Żytkow, A. N. 2012, MNRAS, 421, 2713

Ball, W. H., Tout, C. A., Żytkow, A. N., & Eldridge, J. J. 2011, MNRAS, 414, 2751

Begelman, M. C. 2010, MNRAS, 402, 673

Begelman, M. C., Rossi, E. M., & Armitage, P. J. 2008, MNRAS, 387, 1649

Begelman, M. C., Volonteri, M., & Rees, M. J. 2006, MNRAS, 370, 289

Bovino, S., Latif, M. A., Grassi, T., & Schleicher, D. R. G. 2014, MNRAS, 441, 2181

Bromm, V., & Loeb, A. 2003, ApJ, 596, 34

Bromm, V., Yoshida, N., Hernquist, L., & McKee, C. F. 2009, Nature, 459, 49

Bryan, G. L., et al. 2014, ApJS, 211, 19

Cazaux, S., & Spaans, M. 2009, A&A, 496, 365

Ciardi, B., & Ferrara, A. 2005, Space Sci. Rev., 116, 625

Clark, P. C., Glover, S. C. O., Smith, R. J., Greif, T. H., Klessen, R. S., & Bromm, V. 2011, Science, 331, 1040

Dijkstra, M., Ferrara, A., & Mesinger, A. 2014, ArXiv e-prints:1405.6743

Dijkstra, M., Haiman, Z., Mesinger, A., & Wyithe, J. S. B. 2008, MNRAS, 391, 1961

Grassi, T., Bovino, S., Schleicher, D. R. G., Prieto, J., Seifried, D., Simoncini, E., & Gianturco, F. A. 2014, MNRAS, 439, 2386

Greif, T. H., Bromm, V., Clark, P. C., Glover, S. C. O., Smith, R. J., Klessen, R. S., Yoshida, N., & Springel, V. 2012, MNRAS, 424, 399

Greif, T. H., Johnson, J. L., Klessen, R. S., & Bromm, V. 2008, MNRAS, 387, 1021

Haiman, Z. 2012, ArXiv e-prints:1203.6075

Hirano, S., Hosokawa, T., Yoshida, N., Umeda, H., Omukai, K., Chiaki, G., & Yorke, H. W. 2014, ApJ, 781, 60

Hosokawa, T., Omukai, K., & Yorke, H. W. 2012, ApJ, 756, 93

Hosokawa, T., Yorke, H. W., Inayoshi, K., Omukai, K., & Yoshida, N. 2013, ApJ, 778, 178

Inayoshi, K., Omukai, K., & Tasker, E. J. 2014, ArXiv e-prints:1404.4630

Johnson, J. L., & Khochfar, S. 2011, MNRAS, 413, 1184

Johnson, J. L., Khochfar, S., Greif, T. H., & Durier, F. 2011, MNRAS, 410, 919

Johnson, J. L., Whalen, D. J., Agarwal, B., Paardekooper, J.-P., & Khochfar, S. 2014, ArXiv e-prints:1405.2081

Kamann, S., Wisotzki, L., Roth, M. M., Gerssen, J., Husser, T.-O., Sandin, C., & Weilbacher, P. 2014, ArXiv e-prints:1404.2781

Latif, M. A., Bovino, S., Van Borm, C., Grassi, T., Schleicher, D. R. G., & Spaans, M. 2014a, ArXiv e-prints:1404.5773

Latif, M. A., Niemeyer, J. C., & Schleicher, D. R. G. 2014b, MNRAS, 440, 2969

Latif, M. A., Schleicher, D. R. G., & Schmidt, W. 2014c, MNRAS, 440, 1551

Latif, M. A., Schleicher, D. R. G., Schmidt, W., & Niemeyer, J. 2013a, MNRAS, 433, 1607

—. 2013b, MNRAS, 430, 588

—. 2013c, ApJ, 772, L3

—. 2013d, MNRAS, 432, 668

Latif, M. A., Schleicher, D. R. G., Schmidt, W., & Niemeyer, J. C. 2013e, MNRAS, 436, 2989

Latif, M. A., Schleicher, D. R. G., & Spaans, M. 2012, A&A, 540, A101

Latif, M. A., Schleicher, D. R. G., Spaans, M., & Zaroubi, S. 2011a, A&A, 532, A66

Latif, M. A., Zaroubi, S., & Spaans, M. 2011b, MNRAS, 411, 1659

Lodato, G., & Natarajan, P. 2006, MNRAS, 371, 1813

Maio, U., Khochfar, S., Johnson, J. L., & Ciardi, B. 2011, MNRAS, 414, 1145

Martin, P. G., Schwarz, D. H., & Mandy, M. E. 1996, ApJ, 461, 265

Oh, S. P., & Haiman, Z. 2002, ApJ, 569, 558

Omukai, K. 2001, ApJ, 546, 635

Peters, T., Schleicher, D. R. G., Smith, R. J., Schmidt, W., & Klessen, R. S. 2014, ArXiv e-prints:1406.0346

Prieto, J., Jimenez, R., & Haiman, Z. 2013, ArXiv e-prints-1301.5567

Regan, J. A., & Haehnelt, M. G. 2009, MNRAS, 393, 858

Regan, J. A., Johansson, P. H., & Haehnelt, M. G. 2014, MNRAS, 439, 1160

Safranek-Shrader, C., Agarwal, M., Federrath, C., Dubey, A., Milosavljević, M., & Bromm, V. 2012, MNRAS, 426, 1159

Safranek-Shrader, C., Milosavljević, M., & Bromm, V. 2014, MNRAS, 440, L76

Schleicher, D. R. G., Galli, D., Palla, F., Camenzind, M., Klessen, R. S., Bartelmann, M., & Glover, S. C. O. 2008, A&A, 490, 521

Schleicher, D. R. G., Palla, F., Ferrara, A., Galli, D., & Latif, M. 2013, A&A, 558, A59

Schleicher, D. R. G., Spaans, M., & Glover, S. C. O. 2010, ApJ, 712, L69

Shang, C., Bryan, G. L., & Haiman, Z. 2010, MNRAS, 402, 1249

Spaans, M., & Silk, J. 2000, ApJ, 538, 115

—. 2006, ApJ, 652, 902

Stacy, A., Greif, T. H., & Bromm, V. 2012, MNRAS, 422, 290

Trenti, M., Stiavelli, M., & Michael Shull, J. 2009, ApJ, 700, 1672

Turk, M. J., Smith, B. D., Oishi, J. S., Skory, S., Skillman, S. W., Abel, T., & Norman, M. L. 2011, ApJS, 192, 9

Volonteri, M. 2010, A&A Rev., 18, 279

Volonteri, M., & Bellovary, J. 2012, Reports on Progress in Physics, 75, 124901

Whalen, D. J., Johnson, J. L., Smidt, J., Meiksin, A., Heger, A., Even, W., & Fryer, C. L. 2013a, ApJ, 774, 64

Whalen, D. J., et al. 2013b, ApJ, 768, 195

Wise, J. H., Turk, M. J., & Abel, T. 2008, ApJ, 682, 745

Wolcott-Green, J., Haiman, Z., & Bryan, G. L. 2011, MNRAS, 418, 838

Yue, B., Ferrara, A., Salvaterra, R., Xu, Y., & Chen, X. 2013, MNRAS, 433, 1556

—. 2014, MNRAS

This 2-column preprint was prepared with the AAS LaTeX macros v5.2.